

**1 Distinct functional responses of consumers and their
2 producers to climate drive mutualistic network
3 asymmetry**

4 Gabriel Munoz¹, Paul Savary¹, W. Daniel Kissling², JP Lessard¹

**5 ¹Concordia University,
6 ²University of Amsterdam,**

7 **Abstract**

8 **Aim:** Functional traits are often used to infer the ecological processes that deter-
 9 mine the composition of species assemblages. However, most trait-based approaches
 10 to infer community assembly processes focus on a single trophic level. Owing to the
 11 matching of traits facilitating interactions between resource and consumer assem-
 12 blages, the functional trait diversity of different trophic levels is expected to covary
 13 in space. However, differential response of consumers and producers to environmen-
 14 tal gradients can cause a decoupling of functional diversity between trophic levels,
 15 which we coin functional trophic asymmetry. Here, we develop a metric to quantify
 16 functional trophic asymmetry (FTA) and use it to infer the processes underpinning
 17 multitrophic community assembly, and explore the role of these processes in shaping
 18 the topology of ecological networks.

19 **Location:** Neotropics.

20 **Time period:** Present.

21 **Major taxa:** Mammalian frugivores and palms.

22 **Methods:** We use digitally available data on the functional traits, pairwise mutual-
 23 istic interactions, and geographic distributions of consumers (mammalian frugivores)
 24 and their producers (palms) to quantify functional trophic asymmetry for species
 25 occurring in the Neotropics. To cover major data gaps between species-level trait
 26 and interaction data, we train machine learning models to generate synthetic net-
 27 work data. We then use linear regression models to relate functional asymmetry to
 28 variation in climate, and to assess the influence of functional asymmetry on network
 29 specialization.

30 **Results:** Our approach generated probabilistic networks across 1,072 grid cells in
 31 the Neotropics, revealing networks with a clearly defined modular structure and
 32 substantial differences in their functional richness across trophic levels. Functional
 33 trophic asymmetry increases from regions of the Neotropics with low precipitation
 34 seasonality to regions with high precipitation seasonality. Along this same climatic
 35 gradient, network specialization is positively related to functional trophic asymme-
 36 try.

37 **Main conclusions:** Our results further suggest that mutualistic interactions be-
 38 tween palms and mammals are mediated by matching traits and taxonomic overlap
 39 as a key assembly process at the regional scale. We conclude that increased warming
 40 and seasonal shifts in precipitation caused by global climate change could dispropor-
 41 tionately impact specialist species while increasing functional trophic asymmetry in
 42 ecological networks.

43 **Plain Language Summary**

44 This study explores how differences in functional traits between co-occurring species
 45 assemblages of consumer and producers affect ecological network assembly in the
 46 Neotropics. By focusing on mammalian frugivores and palms as a case study, we de-
 47 veloped a novel metric functional trophic asymmetry (FTA) to measure mismatches
 48 in trait diversity between trophic levels. Using machine learning and statistical mod-
 49 els to augment spatially sparse data on species interactions, we found that FTA
 50 increases in areas with high precipitation seasonality and leads to more specialized
 51 ecological networks. The results suggest that climate change could dispropor-
 52 tionately impact specialist species and increase FTA, altering the structure of species
 53 interactions in these ecosystems.

54 **1 Introduction**

55 Ecologists often examine patterns of functional trait diversity to investigate com-
 56 munity assembly processes (Ackerly, 2003; Kraft et al., 2015). To date, however,
 57 trait-based approaches in ecology often focus on a single trophic level, whereas ap-
 58 proaches that consider multiple trophic levels remain rare (Lavorel et al., 2013;
 59 Seibold et al., 2018). An approach that considers processes operating within and be-
 60 tween trophic levels is necessary to better understand the assembly of multitrophic
 61 communities(Allesina et al., 2008; Marjakangas et al., 2022; Saravia et al., 2022).
 62 Moreover, considering trophic interactions while studying community assembly could
 63 shed new light on processes underpinning ecological networks (Allesina et al., 2008) .

64 Classical approaches to study community assembly rely on the concept of environ-
 65 mental filtering, sorting or selection, where density independent conditions constrain
 66 the functional richness of species assemblages (HilleRisLambers et al., 2012; Kraft
 67 et al., 2015; Laliberté & Legendre, 2010; Villéger et al., 2008). Functional richness
 68 refers to the variability and relative frequency of different functional traits observed
 69 in a community. It is often used to estimate the strength of selection imposed by
 70 the environment (Kraft et al., 2008, 2015; Kraft & Ackerly, 2010). High functional
 71 richness can indicate weak environmental selection whereas low functional richness
 72 can indicate strong selection (Halpern & Floeter, 2008; Kraft et al., 2008; Paine
 73 et al., 2011). In a multitrophic context, the effects of environmental selection can
 74 cascade across trophic levels such that selection on consumer traits can shape the
 75 functional richness of their resources, modulated by their degree of reciprocal de-
 76 pendency or co-evolution (Guzman et al., 2019; Lavorel et al., 2013). Moreover, the
 77 same environmental gradient could exert selective pressures of different strength on
 78 communities at distinct trophic levels (Marjakangas et al., 2022). Differences in the
 79 strength of selective pressure among trophic levels could then possibly constrain the
 80 structure or topologies of trophic networks (Blüthgen et al., 2007; Dehling et al.,
 81 2020; Schleuning et al., 2012).

82 Inferring the relative strength of environmental selection between trophic levels
 83 requires using high-dimensional approaches that are able to deal with sparse ob-
 84 servations for a large number of species (Rohr et al., 2010; Strydom et al., 2022).
 85 We introduce the concept of functional trophic asymmetry (FTA), which allows in-
 86 ferring the relative influence of environmental selection and trait matching on the
 87 composition of multitrophic assemblages ([Figure 1](#)). FTA is the difference in the
 88 richness of interaction-relevant traits between trophic levels in a multitrophic net-
 89 work. FTA can occur because traits mediating species interactions (i.e., interaction
 90 niches) across trophic levels can also mediate the responses of species to their abiotic
 91 environment (i.e. environmental niches) (Dehling et al., 2020; McCain & King, 2014;
 92 Moretti & Legg, 2009; Nagy et al., 2018). As an example, plant seed size determine
 93 the outcome of animal-mediated seed dispersal (Donoso et al., 2017, 2020) as well
 94 as physiological limits, such as tolerances of plant seedlings to desiccation (Hoekstra
 95 et al., 2001). High FTA could indicate differences in the strength of environmental
 96 selection over the interaction niches of distinct trophic levels within a multitrophic
 97 species assemblage. Alternatively, low FTA could indicate that the strength of the
 98 environment selection shaping interaction niches is similar between trophic levels,
 99 e.g. equally weak or equally strong (Marjakangas et al., 2022). When interactions
 100 between producers and consumers are mutualistic, low FTA could also emerge under
 101 strong trait matching and therefore indicate the influence of trait-coevolution during
 102 multitrophic community assembly (Albrecht et al., 2018; Dehling et al., 2014). By
 103 studying spatial variation in functional trophic asymmetry along environmental gra-
 104 dients, we could possibly identify the conditions promoting environmentally versus
 105 cross-trophic interaction- driven community assembly (Bello et al., 2023; Schleuning
 106 et al., 2020).

107 Frameworks linking multitrophic functional diversity to network topology along
 108 broad-scale environmental gradients are crucial to understand the effects of global
 109 change on biodiversity and ecosystem function (Bello et al., 2023; Dehling, 2018;
 110 Schleuning et al., 2014, 2020, 2023). Functional responses of consumer and producer
 111 assemblages to climate influence functional richness at the level of the multitrophic
 112 community (García et al., 2018). Because some of these traits are involved in inter-
 113 actions across trophic levels, the filtering of traits along environmental gradients
 114 could constrain the number of unique interactions and therefore, network topology
 115 (Albrecht et al., 2018; Emer et al., 2020; Marjakangas et al., 2022). As an example,
 116 low multitrophic functional richness could influence emergent patterns in network
 117 structure such as the specialization of multispecies interactions by limiting the rela-
 118 tive availability of interaction partners across trophic levels (Blüthgen et al., 2006,
 119 2007). While high levels of network specialization represent networks predominantly
 120 made of “one-to-one” interactions, low levels of network specialization represent net-
 121 works with species showing predominantly “one-to-many” interactions (Blüthgen et
 122 al., 2006; Blüthgen & Klein, 2011) (Figure 1B). One highly expected outcome is that
 123 when functional trophic asymmetry is high, networks will have low specialization.
 124 For example, take a plant community exhibiting a low richness of flower displays
 125 and which is associated with a bee community (pollinators) exhibiting a wide variety
 126 of proboscis lengths. These plants are unlikely to form “one-to-one” interactions
 127 with only a subset of bee species that have matching proboscis length. Otherwise,
 128 non-matching pollinators would have no food resource and be extirpated. By par-
 129 titioning deviations from expected FTA and network specialization relationships
 130 with null models, one can separate the relative influences of processes operating
 131 between trophic levels (e.g. trait matching) and those within trophic levels (e.g. envi-
 132 ronmental selection) in network assembly (Marjakangas et al., 2022). However, the
 133 relationship between network specialization and functional trophic asymmetry has
 134 not been fully explored.

135 Preserving mutualistic interactions between palms and their mammalian frugivores
 136 is important to sustain biodiversity and ecosystem function in the tropics (Bogoni
 137 et al., 2020; Marques Draxler & Kissling, 2022). Mammalian frugivores facilitate
 138 the dispersal of palm fruits, which helps to prevent local extinctions amid distur-
 139 bance and to maintain biodiversity in these ecological networks (Acevedo-Quintero,
 140 Saldaña-Vázquez, et al., 2020; Dehling, 2018; Messeder et al., 2020). Exploring pat-
 141 terns of co-variation in the functional richness of palm and frugivore assemblages
 142 along environmental gradients is a first step in this direction. Here, we ask (1) which
 143 climatic variable(s) best explains variation in the functional richness of palms vs
 144 mammal frugivores, (2) whether differences in these relationships lead to functional
 145 trophic asymmetry, (3) where does functional asymmetry peaks in the Neotropics
 146 and (4) whether asymmetry relates to network specialization.

147 2 Methods

148 In this study, we investigated the variation of functional trophic asymmetry and
 149 network specialization along climatic gradients by gathering species-level information
 150 on traits, interactions, and distributions from literature, museum specimens, and
 151 field collections. The collected data were then processed to create synthetic networks
 152 across gridded regions of the Neotropics and to calculate functional trophic asymme-
 153 try and network specialization variables, followed by using climate data to explain
 154 the variation in these variables across the Neotropics (Figure S1).

155 2.1 Study system

156 We focused on multitrophic communities of Neotropical palms and their mutual-
 157 istic, seed dispersing, mammalian frugivores. Palms (Plantae:Areceae), being a
 158 keystone plant family in tropical regions (Kissling et al., 2012; Onstein et al., 2017),
 159 provide fruit resources to a wide variety of vertebrate frugivores, including birds and

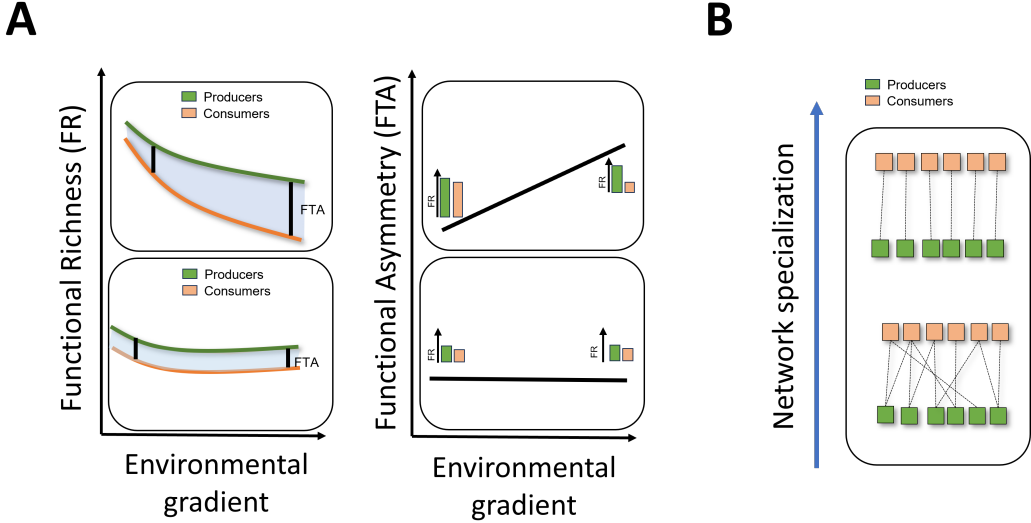


Figure 1: This conceptual model illustrates the dynamic relationship between functional diversity metrics—specifically Functional Richness (FR) and Functional Trait Asymmetry (FTA)—and environmental gradients within ecological networks. The left panel of **Figure A** visualizes the variation in FR for producers (depicted in green) and consumers (depicted in orange) along an environmental gradient. As the environmental gradient intensifies (e.g., through changes in temperature, precipitation, or habitat fragmentation), FR for both producers and consumers generally declines. However, this decline can occur at different rates, leading to two scenarios: (1) **Differential Decline in FR**: If consumer FR declines more sharply than producer FR, a substantial increase in Functional Trait Asymmetry (FTA) occurs. (2) **Parallel Decline in FR**: Alternatively, if both producer and consumer FRs decline at a similar rate, FTA remains relatively constant along the gradient. This scenario indicates a balanced impact of environmental changes across trophic levels, preserving the relative functional relationship between producers and consumers. **Figure B** shifts focus to the implications of changing FTA on network specialization—a measure of how distinct or generalized interactions are between producers and consumers within ecological networks. **Higher Specialization**: This scenario, shown on the left side of the gradient, involves more distinct producer-consumer interactions, where specific consumer species interact with particular producer species. This high specialization often correlates with low FTA, where the functional traits between interacting species are closely aligned. **Lower Specialization**: As environmental stress increases, leading to a higher FTA, the network may shift towards lower specialization. In this state, interactions become more generalized, with consumers utilizing a broader range of producers due to the loss of specific functional traits.

160 mammals (Muñoz et al., 2019; Zona & Henderson, 1989). Frugivore mammals (Ani-
 161 malia:Mammalia) are among the most important palm-seed dispersers, particularly
 162 over long distances. Most frugivore mammals feeding on palms are seed eaters and
 163 pulp eaters, dispersing palm seeds mostly via ectozoochorous dispersal (Messeder et
 164 al., 2020). Importantly, frugivory-related traits have notably underlain palm diver-
 165 sification and played a key role in the evolution of palm traits (Onstein et al., 2014,
 166 2017)

167 **2.2 Data collection**

168 ***2.2.1 Species level geographic distribution data***

169 We obtained binary species distribution data (present/absent) on palms from the
 170 geographic range maps of (Bjørholm et al., 2005) and on mammals from the IUCN
 171 (International Union for the Conservation of Nature) data portal. To generate local
 172 gridded multitrophic species assemblages across the Neotropics, we intersected the
 173 species-level range maps with a spatial grid where each grid cell represented every 1
 174 by 1 degree latitude and longitude change along the extent of the entire Neotropics.
 175 We then listed all palm and mammal frugivore species co-occurring in each grid-cell
 176 as our grid-cell level multitrophic assemblage.

177 ***2.2.2 Species level trait data***

178 We collected species-level multitrophic trait data related to the physiological toler-
 179 ance of palms and frugivorous mammals to the abiotic environment and to their
 180 mutualistic interactions. For palms, we extracted data from the PalmTraits 1.0
 181 dataset (Kissling et al., 2019). We collected data on growth form, maximum stem
 182 height, and average fruit length. For frugivorous mammals, we obtained trait data
 183 from the EltonTraits 1.0 database (Wilman et al., 2014). We selected data on body
 184 mass, diet, and daily activities. Diet data from the EltonTraits 1.0 database is coded
 185 as percentage use distribution across ten diet categories. We excluded from our
 186 analysis species without fruit in their diet. Activity was coded as a dummy variable
 187 with three categories (Diurnal, Crepuscular, Nocturnal). Finally, body mass was
 188 coded as a numerical variable in kg. We excluded bats from the analysis as almost
 189 no Neotropical bat species is feeding on palm fruits (Messeder et al., 2020). In total,
 190 we subset from this dataset the species with available distribution range map, that is
 191 494 palm species and 737 mammal frugivores.

192 ***2.2.3 Pairwise species level interaction data***

193 We used data on seed dispersal interactions between palms and mammals for the
 194 Neotropics, originating from recollections of seed dispersal records found in the pub-
 195 lished literature and interaction records are recorded at the species level (Muñoz et
 196 al., 2019). Each pairwise species interaction record reflects where an article mentions
 197 the fruit or the seed of a palm being dispersed, carried or defecated by a frugivorous
 198 mammal. Interaction records collected in this database were previously vetted to re-
 199 flect effective seed dispersal interactions, while avoiding those that reflect mere seed
 200 consumption (vetting criteria found in: (Muñoz et al., 2019)). In total, we gathered
 201 a total of 581 interaction records between 69 palms and 111 frugivore mammals.

202 ***2.2.4 Grid-cell level environmental data***

203 We used bioclimatic variables from WorldClim (Fick & Hijmans, 2017) to represent
 204 large-scale spatial and temporal variation of climate in the Neotropics. Specifically,
 205 we used mean annual temperature (BIO01), total annual precipitation (BIO12), tem-
 206 perature seasonality (BIO04) and precipitation seasonality (BIO15). Using a moving
 207 window, we compute simple averages for every set of bioclimatic records at each grid
 208 cell, thereby re-scaling the spatial resolution of bioclimatic variables to 1 by 1 de-
 209 gree grid resolution from their original resolution (1 by 1 km²) to match the spatial
 210 resolution of our grid cell species-level data.

211 **2.2.5 Continental level biogeographical data**

212 The Neotropics is a region with a rich evolutionary history which significantly influenced patterns of species colonization and extinction across neotropical plant
 213 and animal species (Antonelli & Sanmartín, 2011; Whiteman-Jennings, 2015) . The
 214 biogeographic regionalization patterns of (Morrone, 2014) distinguish seven major
 215 biogeographic regions (i.e., biogeographic dominions), we use them to delineate the
 216 spatial extent of species pools when simulating network assembly processes.
 217

218 **2.3 Statistical analyses**

219 **2.3.1 A probabilistic continental metaweb**

220 Here, we fitted latent variable models that vary in their assumptions to estimate
 221 interaction probabilities from observed binary data on species interactions. Specifically:
 222 the stochastic block model (SBM), the connectance model, the trait-matching
 223 model, and the matching-centrality model (Terry & Lewis, 2020). The SBM as-
 224 sumes that ecological networks are modular, with species interacting more within
 225 their groups, and outputs an two incidence matrix for palm and mammal species
 226 group affiliations, and a squared matrix (Theta matrix) for interaction probabili-
 227 ties. The connectance model posits that interactions of specialist species are subsets
 228 of those of generalist species, optimizing connectivity scores to recreate observed
 229 network patterns. The trait-matching model assumes non-random species interac-
 230 tions determined by trait differences, optimizing parameters along latent-trait axes.
 231 The matching-centrality model combines connectivity scores and latent-trait axes
 232 (Terry & Lewis, 2020). We fitted these models to our available interaction data
 233 and selected the model that best predicted the observed continental pattern of seed
 234 dispersal interactions. Using Youden's J as a metric that balanced model sensitiv-
 235 ity and specificity (Poisot, 2023), we find that SBM was the best supported model
 236 (Figure S2 A-C). Additional details about the model assumptions are explained in
 237 *Supplementary Text S1*.

238 **2.3.2 Downscaling the continental metaweb to generate grid-cell level
 239 networks**

240 The digitally availability of primary biodiversity data on palms and their mam-
 241 malian frugivores was imbalanced, with well covered data in terms of distribution
 242 ranges, followed by well covered data on species traits, to a limited number of inter-
 243 action records. Therefore, to downscale our initial metaweb to include interactions
 244 between every potentially co-occurring palms and mammal frugivore at
 245 every gridcell of the Neotropics, we use a two fold approach. First, we employed
 246 multinomial logistic regression models that aimed to predict the species level SBM
 247 model results (i.e. group affiliations) from species-level trait data. We justify the
 248 choice of multinomial logistic regression models as these can handle the prediction
 249 of non-binary outcomes, that is in our case, the labeling of SBM groupings per
 250 species. We fitted separate multinomial models for palms and mammal frugivores
 251 using a label backpropagation algorithm and a neural network engine, with 75%
 252 of the data allocated for training and the 25% remaining for testing. We used neu-
 253 ral networks because they are useful when dealing with multicollinearity, as they
 254 can learn complex and non-linear relationships and interactions among predictor
 255 variables. This allowed us to separate the relative importance of distinct matching
 256 traits on SBM group affiliations. We extracted variable importance scores based on
 257 the combinations of the absolute values of the best fit model weights (Gevrey et al.,
 258 2003). Second, we considered as local pairwise species interaction probabilities as
 259 the product of the values from the Theta matrix from the SBM model that repre-
 260 sent the latent interaction probabilities between species pairs within and between
 261 groups multiplied by their probability of co-occurrence (POC) in a gridcell. To rep-
 262 resent species' co-occurrence probabilities, we used the reciprocal distance between
 263 the centroids of species pair ranges within the grid-cell, divided by the sum of its
 264 range areas within the grid-cell. This implied that within each grid cell, species with

265 closer range centroids and larger cumulative areas are more likely to co-occur and
 266 interact. This approach allowed us to recreate synthetic probabilistic plant-mammal
 267 frugivore networks for each grid-cell across the Neotropics, while accounting for the
 268 heterogeneity of species ranges within each grid.

269 ***2.3.3 Measuring Functional Trophic Asymmetry (FTA) and Network*** 270 ***Specialization (H2')***

271 We computed Functional Trophic Asymmetry (FTA) from the results of the SBM
 272 model fit. Specifically, from the matrices representing the incidence of palm or
 273 mammal frugivore species in one of the SBM groupings. Thus, as our measure of
 274 functional richness, we calculated the number of species of each taxon across SBM
 275 groups per grid. Because we had differences in the total number of palm and mam-
 276 mal species across grids, we normalized species counts within gridcells. We then
 277 computed the absolute difference between trophic levels to obtain a measure of FTA
 278 for each combination of SBM groups. Because we had the potential for each palms
 279 and mammals species at each grid to become affiliated to any of 7 SBM groups, and
 280 to interact with any species of the opposite trophic level within and between groups,
 281 we obtained a total of 49 independent FTA measures for each gridcell, one for each
 282 palm-mammal group combination.

283 We measured network specialization at each grid cell using the metric H2'. H2' is
 284 a network-level index that describes the degree of specialization of interactions be-
 285 tween species (Blüthgen et al., 2007). High values indicate networks that are more
 286 specialized, meaning that specialist species from one trophic level interact with spe-
 287 cialist species from the opposite trophic level. Low H2' values indicate networks
 288 among generalists, meaning that there is a low specificity of interactions between
 289 species across trophic levels. Because inferred networks varied in their network size
 290 (i.e., number of unique interactions between palms and mammals), we rarefied the
 291 computation of H2' to networks of the same absolute size per gridcell, resampling
 292 networks to the same number of pairwise interactions (100) at each grid-cell 999
 293 times (Terry & Lewis, 2020). We selected the median of this H2' distribution as our
 294 gridcell level measure of network specialization.

295 We assessed the deviance of ‘observed’ FTA and H2' from null models that simu-
 296 lated stochastic community assembly processes (Dormann et al., 2009). We created
 297 these null models by constructing networks of interactions between a randomized
 298 set of palms and mammals for each gridcell and computing expected values of FTA
 299 and H2'. To do this for a given gridcell, we identified their biogeographic domain
 300 (from (Morrone, 2014)) and randomly sampled 10 palm and mammal species, en-
 301 suring each species is selected only once. To this subsampled species set, we used
 302 the same procedures to calculate FTA and H2' and replicated the process 999 inde-
 303 pendent times to obtain a distribution of expected FTA and H2' values. Finally, we
 304 computed the deviance between observed and expected values with Z-scores.

305 ***2.3.4 Assessing the influence of climate in Functional Trophic Asymme-*** 306 ***try***

307 We fitted linear regression models to investigate the influence of climate to Func-
 308 tional Trophic Asymmetry. We used FTA z-scores as response variables and the
 309 four climatic predictor variables: Mean Annual Temperature (Temp), Total Annual
 310 Precipitation (Prec), Temperature Seasonality (TS), and Precipitation Seasonality
 311 (PS) as predictor variables. In addition, we included the identity of the SBM palm-
 312 mammal group combination as an interaction term. Prior to fitting the models, we
 313 scale-transformed the climatic variables such that they all share the same mean but
 314 only differ in their standard deviation.

315 **2.3.5 Assessing the influence of Functional Trophic Asymmetry in Net-**
 316 **work Specialization**

317 We fitted linear regression models to investigate the effects of Functional Trophic
 318 Asymmetry in Network specialization. We used the average (mean) and standard
 319 deviation (sd) of FTA across all gridcells and SBM combinations as our predictor
 320 variables. By including both as predictors, the model accounts for not only the over-
 321 all asymmetry but also its distribution among SBM groupings. We used the rarefied
 322 gridcell records of H2' as our response variable. To asses model significance, we com-
 323 pared the estimates of this model to a distribution of expected model coefficients
 324 from fitting the same linear model for each of the null network assembly replicates.

325 **3 Results**

326 **3.1 The structure of mutualistic networks between palms and their**
 327 **mammalian frugivores across the Neotropics**

328 The SBM model organized the continental set of palm and mammal species into a
 329 matrix sorting species into seven SBM groups and an accompanying matrix that
 330 quantified interaction probabilities between and within groups. In our model, there
 331 was a 1.74 fold increase in the likelihood of interactions between species within SBM
 332 groups rather than between SBM groups (Figure 2A). For palms, important trait
 333 variables that predicted SBM group affiliation were palm fruit length, maximum
 334 stem height, and palm growth form (*Acaulescent* or *Erect*) (Figure S3-A). For mam-
 335 mals, important trait variables to predict species group affiliations were mammal
 336 activity, the logarithm of the *body mass*, and percentage of frugivory on diet as pre-
 337 dictor variables (Figure S3-B). These analysis revealed that SBM group assortments
 338 represent communities of palms (Figure S4) and mammal frugivores (Figure S5)
 339 with unique trait combinations within the high-dimensional multitrophic spectrum
 340 of interaction-relevant traits. Our approach to downscale a continental metaweb was
 341 able to generate probabilistic networks between palms and mammalian frugivores
 342 for 1,072 grid cells acrossss the Neotropics. Each network had in average nine interac-
 343 tion partners per species (sd = 5.62), 27 mammals per grid cell (sd = 14.97), and 11
 344 palms per grid cell (sd = 11.42).

345 **3.2 Differences in trait-climate relationships across trophic levels lead to**
 346 **Functional Trophic Asymmetry**

347 FTA z-scores (Figure 2B) indicate that in average FTA was less than the FTA ex-
 348 pected from a null assembly model. Out of the 49 SBM group combinations, those
 349 with less than expected asymmetries are generally between palms in groups 1, 2,
 350 and 5 and mammals in groups 6 and 3. Conversely, combinations with significantly
 351 greater than expected asymmetries are generally found between palms in SBM
 352 groups 6 and 4 and mammals in SBM groups 1, 2, and 5. FTA peaks in tropical and
 353 mountainous regions while being lower in more temperate areas of the Neotropics,
 354 and remains stable throughout tropical and humid regions (Figure 2A). The results
 355 of our linear model shows significant differences in FTA among SBM groups. In
 356 addition, it shows a relationship between the spatial variation of climate and FTA.
 357 However, the significance and direction of effects vary as a function of the SBM
 358 group combinations (Figure 3B, Table 1). While the overall fixed model estimates
 359 do not show significant effects of climatic variation in FTA across all SBM group
 360 combinations [Temp (Mean annual temperature) (= 0.0051, p=0.859), Prec (To-
 361 tal annual precipitation) (= -0.0364 p=0.384), TS (Temperature Seasonality) (=
 362 -0.0180 p=0.746), and PS (Precipitation Seasonality) (= -0.0507 p=0.250)];
 363 for specific group combinations, FTA is significantly predicted by climate, partic-
 364 ularly by changes in Precipitation Seasonality (Figure S6). Approximately 59% of
 365 the variability in the FTA z-score is explained by the linear model with our climate
 366 predictors as fixed effects and SBM group identity as interaction terms (adjusted
 367 R-squared = 0.59).

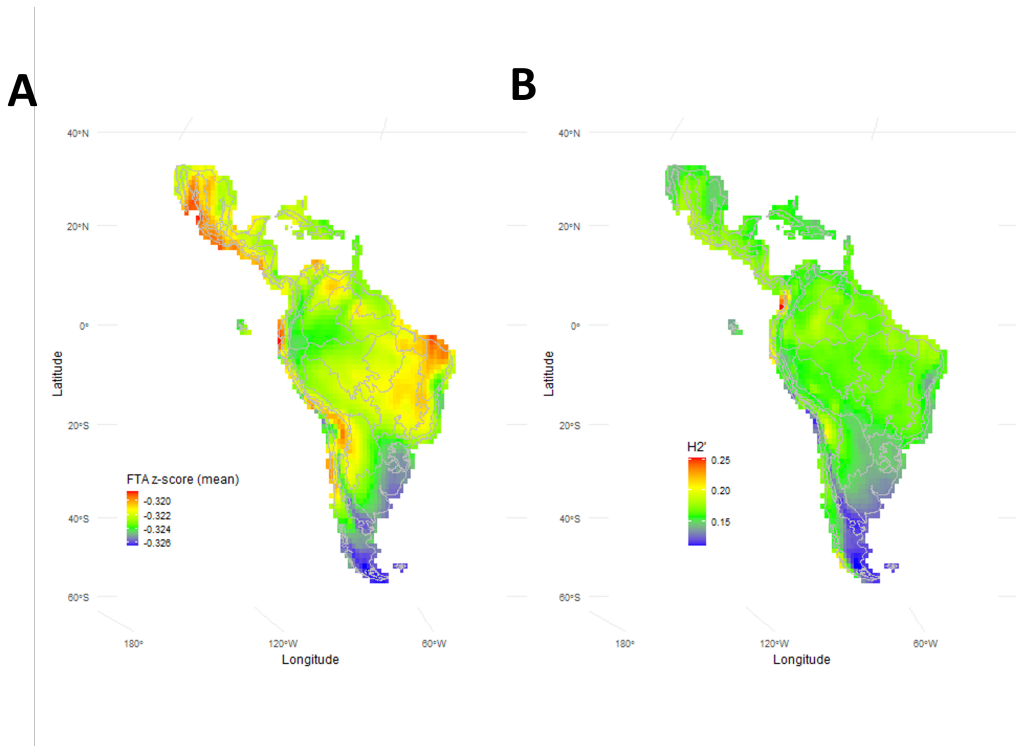


Figure 2: Spatial distribution of (A) FTA z-score (mean) and (B) $H2'$ network specialization index across the Neotropics. Panel A depicts the geographic variation in the mean z-scores of the Functional Trophic Asymmetry (FTA). Areas with higher z-scores indicate greater asymmetry in the richness of interaction relevant traits between trophic levels, whereas lower scores suggest more balanced trait distributions. Panel B presents the spatial distribution the degree of species specialization of interactions within ecological networks. This panel reveals significant latitudinal gradients, particularly marked in the Andes and the Southern Cone.

368 On one hand, group combinations exhibiting a positive relationship between FTA
 369 and precipitation seasonality are characterized by a relatively stable functional richness
 370 of mammals across gradients of precipitation seasonality, while the functional
 371 richness of palms increases under these conditions (Figures S6, S7). A significant
 372 portion of this pattern can be attributed to turnover within the palm community
 373 of SBM group 6, which predominantly consists of small to medium-sized drupes or
 374 berries. These palms, which belong to genera such as *Acrocomia*, *Allagoptera*, and
 375 *Astrocaryum* are typically of tropical origin and display diverse growth forms, includ-
 376 ing both erect and acaulescent. Conversely, group combinations showing a negative
 377 association between FTA and precipitation seasonality are primarily driven by pat-
 378 terns in the palm community of SBM group 5 (Figures S6, S7). In this scenario,
 379 while the functional richness of mammals remains stable, the functional richness of
 380 these palms, generally characterized by species with erect growth forms and large
 381 fruits, increases in regions with low precipitation seasonality.

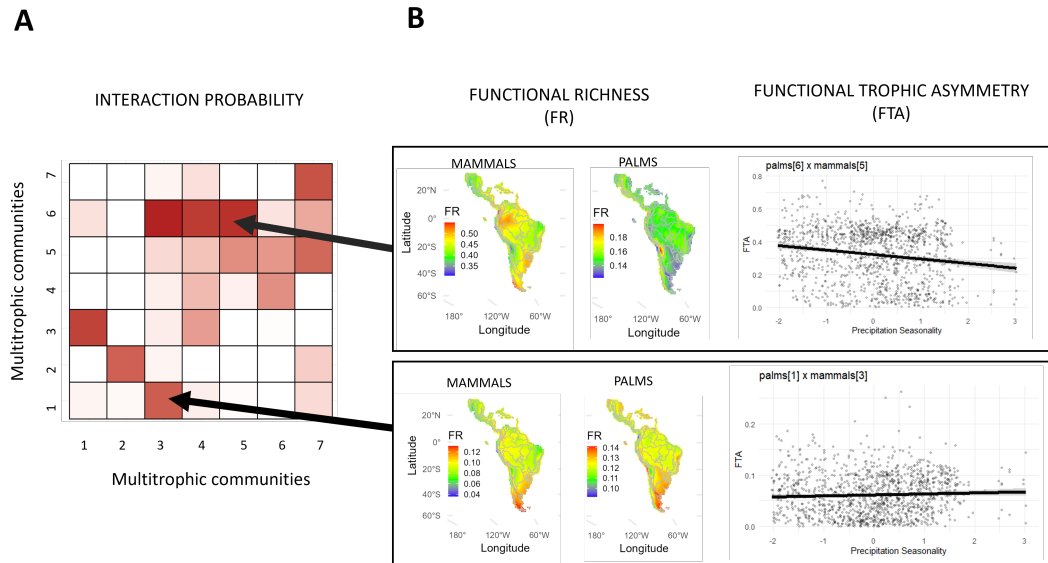


Figure 3: Figure 3: **(A)** Heatmap depicting the interaction probability among various multitrophic communities across different SBM (Stochastic block model) groups. The intensity of red shading correlates with the strength of these interactions, where darker shades signify higher probabilities of interaction between species within or between SBM groups. **(B)** The left panels present geographical maps illustrating the distribution of FR for both mammals and palms, identifying regions with distinct levels of functional diversity for a given multitrophic combination of species at one SBM group pair. The right panels illustrate the significant relationship observed between FTA and precipitation seasonality.

3.3 Functional Trophic Asymmetry increases Network Specialization

We found overall, palm-mammalian frugivore networks had low specialization, H_2' ranged from 0.12 to 0.25. In addition, there was a significant relationship between aggregated gridcell records of Functional Trophic Asymmetry and H_2' metric. Specifically, FTA z-scores increased H_2' by 3.28 units per mean unit increase across all SBM groups. Additionally, the standard deviation of FTA z-scores decreased H_2' by 1.01 units per unit increase across all SBM groups (SD FTA). While this linear model explained only around 8.7% of the total spatial variability in H_2' (adjusted

390 R-squared = 0.087), the results of our simulations show that the intercept and slope
 391 estimates are statistically significant from null assembly models (Figure S7).

392 4 Discussion

393 By making use of digitally available primary biodiversity data at broad scales, our
 394 approach provides novel insights into the assembly of mutualistic networks. By iden-
 395 tifying species clusters of palms and mammals with similar interaction patterns, we
 396 offer a more nuanced understanding of network assembly dynamics within these mul-
 397 titrophic communities. The distribution of Functional Trophic Asymmetry (FTA)
 398 across different climatic regions of the Neotropics underscores the importance of con-
 399 temporary climate change in shaping interaction niches across species' distributional
 400 ranges, with precipitation seasonality emerging as a key predictor of FTA for certain
 401 SBM palm and mammal group combinations, where higher FTA increase overall
 402 network specialization.

403 The delineation of interactions into distinct groups indicates that, at a continen-
 404 tal scale, the network of seed dispersal interactions is highly compartmentalized.
 405 This finding aligns with previous work reporting significant modularity in palm
 406 seed dispersal interactions across the Neotropical continent (Muñoz et al., 2019).
 407 In our study, we extend this understanding by identifying palm growth form and
 408 mammal foraging activity periods as key palm and animal traits driving this broad
 409 scale modularity through changes in functional richness. Clusters of similarly inter-
 410 acting species obtained from SBM models such as ours have been shown to reflect
 411 spatio-temporal segregation of species assemblages and the differentiation of interac-
 412 tion niches (Durand-Bessart et al., 2023). The observed distribution of interaction
 413 probabilities within and between SBM groups highlights multitrophic assemblages
 414 being central to the entire metaweb, notably the palm and mammal species in SBM
 415 groups 5 and 6, which are those with extensive distributional ranges and more gen-
 416 eralist diets. Conversely, it also identifies peripheral groups, such as species in SBM
 417 groups 1-3, which exhibit narrower interaction niches. These peripheral species as-
 418 semblages may correspond to those species with restricted ranges or specialized diets.
 419 Indeed, SBM groups 5-6 include larger, nocturnal mammals that feed on palms with
 420 varying fruit sizes and growth forms, ranging from erect to acaulescent, whereas
 421 SBM groups 1-3 predominantly consist of smaller, diurnal mammals that consume
 422 small fruits from erect palms.

423 Our linear model highlights Precipitation Seasonality as a key factor predicting the
 424 Functional Trophic Asymmetry (FTA) in key SBM groupings. This suggests that
 425 spatial variation in interaction niches emerges from the differences in the strength of
 426 environmental selection between trophic levels. Such uneven pressures result in mul-
 427 titrophic assemblages where not all co-occurring trait combinations align optimally
 428 with the global preferences between species interaction partners, thus contributing
 429 to promote structural diversity in seed dispersal networks across Neotropical sites.
 430 For example in SBM groups 1-3, mammalian frugivores, which can exhibit a broad
 431 tolerance for varying levels of precipitation seasonality, may predominantly consume
 432 small-fruited palms in regions with high precipitation seasonality. This is likely be-
 433 cause palms with smaller fruits are better adapted to thrive under conditions of vari-
 434 able water availability. Consequently, increased aridity (e.g. due to climate change)
 435 is expected to result in increased FTA, driven by the restricted functional richness of
 436 available resources for consumers. In SBM groups 5-6, palms with larger fruit sizes
 437 and predominantly erect growth forms consumed by large sized frugivores might re-
 438 flect adaptations to attract high quality animal seed disperses in environments where
 439 consistent water availability promotes higher habitat complexity and plant competi-
 440 tion. Consequently, increased aridity is expected to result in increased FTA, but this
 441 time driven by the restricted functional richness of available consumers relative to
 442 producers. In both cases, FTA imposes limits over trait matching between partners

443 of distinct trophic levels and the partitioning of interaction niches within species of
 444 the same trophic level.

445 The a low degree of specialization observed for palm-mammal frugivore seed dis-
 446 persal networks is not entirely unexpected given the historical ecological shifts that
 447 these species have experienced in the Neotropics. Unlike other major tropical re-
 448 gions, such as the Afrotropics and South-East Asia, the Neotropics had significant
 449 post-Pleistocene extinctions, which heavily altered mammalian communities. These
 450 extinctions, which impacted disproportionately to mammal megafauna, likely ex-
 451 acerbate competition and extinction rates among their large-fruited palm partners,
 452 particularly in those regions with high mammal diversity and endemism. (Webb,
 453 2006; **whiteman2015?**) Concurrently, the radiation of small-fruited palm taxa
 454 (Onstein et al., 2014, 2017) further contributed to the decoupling of trait diversity
 455 between palms and mammals and the re-structuring of seed dispersal networks
 456 across trophic levels in the Neotropics. Without this trait decoupling due the co-
 457 evolution dynamics between palms and mammal frugivores may have remained
 458 unaltered, fostering otherwise more specialized networks.

459 The positive estimate for mean FTA suggests a strong positive influence of FTA on
 460 H2', thus promoting network specialization. In contrast, the negative estimate for
 461 FTA standard deviation (SD) indicates that a large variation in FTA within SBM
 462 group combinations significantly reduces H2', implying more generalist interactions.
 463 This suggest, that while overall higher FTA promotes network specialization, an
 464 inconsistent FTA across SBM groups can disrupt this pattern, making network struc-
 465 ture less predictable from multitrophic trait patterns. Previous research in insular re-
 466 gions where trophic communities are often subject to asymmetric filtering strengths
 467 have shown that the specialization of mutualistic networks can indeed be resilient
 468 to shifts in the degree of ecological filters between trophic levels. Particularly, if the
 469 networks are well supported by generalist species (Schleuning et al., 2012, 2016). It
 470 is therefore critical to consider changes in the underlying network structure when
 471 evaluating potential effects that climate-driven species or species trait losses have in
 472 ecosystem function Classen et al. (2020)

473 We validated the statistic significance of the model parameters through null simu-
 474 lations of network assembly,. However, it is noteworthy that our null models are
 475 limited to presence/absence permutations. Therefore, the potential influence of vary-
 476 ing species relative abundances across sites was not considered in this study. It is
 477 well established that population-density dependent effects can modify interaction
 478 probabilities from trait matching and range co-occurrences (Donoso et al., 2017;
 479 McFadden et al., 2022; Peña et al., 2023). Future studies should aim to incorpo-
 480 rate species abundance estimates when defining interaction probabilities. However,
 481 despite ongoing efforts, such data is not readily available for multiple species at dif-
 482 ferent trophic levels, and at broad spatial scales. Our results help elucidate mecha-
 483 nisms that contribute towards a broader theory of multitrophic community assembly.
 484 However, given the current limitation in obtaining reliable species abundance data,
 485 we advise caution when utilizing our data pipelines for making finer-scale spatial
 486 predictions of network assembly and interaction diversity. Similarly, the use bio-
 487 geographic domains to delineate the species pools in the construction of our null
 488 models respects ecological theory and considers both historical and regional species
 489 pools (Carstensen et al., 2013; Cornell & Harrison, 2014; McFadden et al., 2022).
 490 However, one critical assumption of this approach is that species within each bio-
 491 geographic dominion are all equally likely to colonize a given community (Lessard
 492 et al., 2012) While this assumption may simplify the computational complexity of
 493 our algorithms, future work could penalize dispersal distances with landscape level
 494 variables such as the slope terrain (Préau et al., 2022; Schlägel et al., 2020). Finally,
 495 the clustering of interactions captured by the SBM may be also capturing reveal
 496 relatively unexplored drivers of interaction assembly, such as phylogenetic niche con-

497 servatism (Ackerly, 2003; Pyron et al., 2015; Wiens & Graham, 2005), where closely
 498 related species retain similar ecological traits over evolutionary time, and/or the
 499 widespread extinctions of large mammals frugivores and the rapid trait speciation
 500 of small fruited palms (Donoso et al., 2020; Lim et al., 2020; Onstein et al., 2017)
 501 . Partitioning these aspects and their relative influences in delineating SBM group
 502 assignments can be future research avenues to better understand the underlying
 503 mechanisms behind mutualistic interaction patterns in space and time.

504 Unraveling the complexity of network assembly processes across broad spatial scales
 505 requires continuous development and refining of statistical workflows and biodiversity
 506 data pipelines that integrate digitally available data from diverse sources (Kissling
 507 et al., 2012; Thuiller et al., 2024). Continued field collection, their open-release,
 508 and data standardization is crucial if we want to expand our capacity to training
 509 models capable of predicting ecological network structures at a global scale with a
 510 high degree of spatial and/or temporal resolution(Poisot et al., 2016, 2021). While
 511 many of these modelling approaches are in early development, their success hinges
 512 on the availability and reliability of foundational data. We have demonstrated that
 513 with sparse data across large scales, novel models can indeed be developed. Filling
 514 global data gaps and leveling data completeness across species ranges, traits, and
 515 interactions can certainly enhance predictive accuracy. While our case study has a
 516 history of digitally available natural history data on both palms and mammal frugi-
 517 vores, such comprehensive datasets are not available for many other tropical clades.
 518 We thus advocate for increased awareness, action, and funding for global biodiver-
 519 sity programs that collect and digitize natural records, thus enabling the continuous
 520 development of large-scale spatially explicit predictive models that inform about
 521 mechanisms of network assembly, and their relationship to climate and ecosystem
 522 function.

523 5 Tables

524 Table 1: Linear regression analysis of the relationship between Bioclimatic Predic-
 525 tors (Mean Annual Temperature, Total Annual Precipitation, Precipitation Season-
 526 ality, Temperature Seasonality) and Functional Trophic Asymmetry within SBM
 527 groups (p1m1 - p7m7). Statistically significant effects ($p < 0.05$) are marked with (*).
 528 Beta correspond to the variable effect coefficient in the model and SE correspond to
 529 the standard error.

Characteristic	Beta ¹	SE ²
Mean Annual Temperature	0.01	0.029
SBM group		
p1m1	—	—
p1m2	-0.65***	0.035
p1m3	-0.50***	0.035
p1m4	0.00	0.035
p1m5	-1.5***	0.035
p1m6	0.57***	0.035
p1m7	0.00	0.035
p2m2	0.77***	0.035
p2m3	0.42***	0.035
p2m5	-2.0***	0.035
p2m6	0.84***	0.035
p3m1	-1.4***	0.035
p3m2	-1.7***	0.035
p3m3	-1.5***	0.035
p3m4	-1.4***	0.035
p3m5	-0.22***	0.035

p3m6	-1.8***	0.035
p3m7	-1.4***	0.035
p4m1	0.15***	0.035
p4m2	-0.12***	0.035
p4m3	-0.59***	0.035
p4m4	0.15***	0.035
p4m5	-1.8***	0.035
p4m6	0.47***	0.035
p4m7	0.15***	0.035
p5m2	0.77***	0.035
p5m3	0.42***	0.035
p5m5	-2.0***	0.035
p5m6	0.84***	0.035
p6m1	1.5***	0.035
p6m2	0.03	0.035
p6m3	0.02	0.035
p6m4	1.5***	0.035
p6m5	-2.7***	0.035
p6m6	-0.01	0.035
p6m7	1.5***	0.035
p7m1	0.37***	0.035
p7m2	-0.45***	0.035
p7m3	-0.22***	0.035
p7m4	0.37***	0.035
p7m5	-1.9***	0.035
p7m6	0.43***	0.035
p7m7	0.37***	0.035
Total Annual Precipitation	-0.04	0.042
Temperature Seasonality	-0.02	0.056
Precipitation Seasonality	-0.05	0.044
Mean Annual Temperature * SBM group		
Mean Annual Temperature * p1m2	0.01	0.040
Mean Annual Temperature * p1m3	-0.01	0.040
Mean Annual Temperature * p1m4	0.00	0.040
Mean Annual Temperature * p1m5	-0.01	0.040
Mean Annual Temperature * p1m6	0.04	0.040
Mean Annual Temperature * p1m7	0.00	0.040
Mean Annual Temperature * p2m2	0.02	0.040
Mean Annual Temperature * p2m3	-0.06	0.040
Mean Annual Temperature * p2m5	-0.01	0.040
Mean Annual Temperature * p2m6	0.02	0.040
Mean Annual Temperature * p3m1	0.05	0.040
Mean Annual Temperature * p3m2	0.04	0.040
Mean Annual Temperature * p3m3	0.06	0.040
Mean Annual Temperature * p3m4	0.05	0.040
Mean Annual Temperature * p3m5	0.05	0.040
Mean Annual Temperature * p3m6	0.06	0.040
Mean Annual Temperature * p3m7	0.05	0.040
Mean Annual Temperature * p4m1	-0.05	0.040
Mean Annual Temperature * p4m2	0.08	0.040
Mean Annual Temperature * p4m3	0.00	0.040
Mean Annual Temperature * p4m4	-0.05	0.040
Mean Annual Temperature * p4m5	0.01	0.040
Mean Annual Temperature * p4m6	0.05	0.040
Mean Annual Temperature * p4m7	-0.05	0.040

Mean Annual Temperature * p5m2	0.02	0.040
Mean Annual Temperature * p5m3	-0.06	0.040
Mean Annual Temperature * p5m5	-0.01	0.040
Mean Annual Temperature * p5m6	0.02	0.040
Mean Annual Temperature * p6m1	-0.05	0.040
Mean Annual Temperature * p6m2	0.06	0.040
Mean Annual Temperature * p6m3	0.03	0.040
Mean Annual Temperature * p6m4	-0.05	0.040
Mean Annual Temperature * p6m5	0.01	0.040
Mean Annual Temperature * p6m6	0.05	0.040
Mean Annual Temperature * p6m7	-0.05	0.040
Mean Annual Temperature * p7m1	-0.03	0.040
Mean Annual Temperature * p7m2	0.08*	0.040
Mean Annual Temperature * p7m3	0.01	0.040
Mean Annual Temperature * p7m4	-0.03	0.040
Mean Annual Temperature * p7m5	0.00	0.040
Mean Annual Temperature * p7m6	0.04	0.040
Mean Annual Temperature * p7m7	-0.03	0.040
SBM group * Total Annual Precipitation		
p1m2 * Total Annual Precipitation	0.01	0.059
p1m3 * Total Annual Precipitation	-0.05	0.059
p1m4 * Total Annual Precipitation	0.00	0.059
p1m5 * Total Annual Precipitation	0.10	0.059
p1m6 * Total Annual Precipitation	-0.08	0.059
p1m7 * Total Annual Precipitation	0.00	0.059
p2m2 * Total Annual Precipitation	0.04	0.059
p2m3 * Total Annual Precipitation	0.10	0.059
p2m5 * Total Annual Precipitation	0.10	0.059
p2m6 * Total Annual Precipitation	-0.06	0.059
p3m1 * Total Annual Precipitation	0.04	0.059
p3m2 * Total Annual Precipitation	0.04	0.059
p3m3 * Total Annual Precipitation	0.02	0.059
p3m4 * Total Annual Precipitation	0.04	0.059
p3m5 * Total Annual Precipitation	-0.11	0.059
p3m6 * Total Annual Precipitation	0.05	0.059
p3m7 * Total Annual Precipitation	0.04	0.059
p4m1 * Total Annual Precipitation	0.03	0.059
p4m2 * Total Annual Precipitation	0.00	0.059
p4m3 * Total Annual Precipitation	-0.06	0.059
p4m4 * Total Annual Precipitation	0.03	0.059
p4m5 * Total Annual Precipitation	0.10	0.059
p4m6 * Total Annual Precipitation	-0.06	0.059
p4m7 * Total Annual Precipitation	0.03	0.059
p5m2 * Total Annual Precipitation	0.04	0.059
p5m3 * Total Annual Precipitation	0.10	0.059
p5m5 * Total Annual Precipitation	0.10	0.059
p5m6 * Total Annual Precipitation	-0.06	0.059
p6m1 * Total Annual Precipitation	0.11	0.059
p6m2 * Total Annual Precipitation	0.02	0.059
p6m3 * Total Annual Precipitation	0.07	0.059
p6m4 * Total Annual Precipitation	0.11	0.059
p6m5 * Total Annual Precipitation	0.06	0.059
p6m6 * Total Annual Precipitation	-0.10	0.059
p6m7 * Total Annual Precipitation	0.11	0.059
p7m1 * Total Annual Precipitation	0.02	0.059

p7m2 * Total Annual Precipitation	-0.03	0.059
p7m3 * Total Annual Precipitation	0.06	0.059
p7m4 * Total Annual Precipitation	0.02	0.059
p7m5 * Total Annual Precipitation	0.10	0.059
p7m6 * Total Annual Precipitation	-0.05	0.059
p7m7 * Total Annual Precipitation	0.02	0.059
SBM group * Temperature Seasonality		
p1m2 * Temperature Seasonality	0.01	0.079
p1m3 * Temperature Seasonality	0.13	0.079
p1m4 * Temperature Seasonality	0.00	0.079
p1m5 * Temperature Seasonality	0.02	0.079
p1m6 * Temperature Seasonality	0.16*	0.079
p1m7 * Temperature Seasonality	0.00	0.079
p2m2 * Temperature Seasonality	0.01	0.079
p2m3 * Temperature Seasonality	-0.10	0.079
p2m5 * Temperature Seasonality	0.01	0.079
p2m6 * Temperature Seasonality	0.10	0.079
p3m1 * Temperature Seasonality	0.03	0.079
p3m2 * Temperature Seasonality	0.04	0.079
p3m3 * Temperature Seasonality	0.08	0.079
p3m4 * Temperature Seasonality	0.03	0.079
p3m5 * Temperature Seasonality	0.17*	0.079
p3m6 * Temperature Seasonality	0.04	0.079
p3m7 * Temperature Seasonality	0.03	0.079
p4m1 * Temperature Seasonality	-0.02	0.079
p4m2 * Temperature Seasonality	-0.02	0.079
p4m3 * Temperature Seasonality	0.05	0.079
p4m4 * Temperature Seasonality	-0.02	0.079
p4m5 * Temperature Seasonality	0.02	0.079
p4m6 * Temperature Seasonality	0.12	0.079
p4m7 * Temperature Seasonality	-0.02	0.079
p5m2 * Temperature Seasonality	0.01	0.079
p5m3 * Temperature Seasonality	-0.10	0.079
p5m5 * Temperature Seasonality	0.01	0.079
p5m6 * Temperature Seasonality	0.10	0.079
p6m1 * Temperature Seasonality	0.09	0.079
p6m2 * Temperature Seasonality	0.10	0.079
p6m3 * Temperature Seasonality	0.14	0.079
p6m4 * Temperature Seasonality	0.09	0.079
p6m5 * Temperature Seasonality	-0.04	0.079
p6m6 * Temperature Seasonality	0.07	0.079
p6m7 * Temperature Seasonality	0.09	0.079
p7m1 * Temperature Seasonality	-0.01	0.079
p7m2 * Temperature Seasonality	0.06	0.079
p7m3 * Temperature Seasonality	0.03	0.079
p7m4 * Temperature Seasonality	-0.01	0.079
p7m5 * Temperature Seasonality	0.01	0.079
p7m6 * Temperature Seasonality	0.11	0.079
p7m7 * Temperature Seasonality	-0.01	0.079
SBM group * Precipitation Seasonality		
p1m2 * Precipitation Seasonality	-0.05	0.062
p1m3 * Precipitation Seasonality	0.12*	0.062
p1m4 * Precipitation Seasonality	0.00	0.062
p1m5 * Precipitation Seasonality	-0.06	0.062
p1m6 * Precipitation Seasonality	0.49***	0.062

p1m7 *	Precipitation Seasonality	0.00	0.062
p2m2 *	Precipitation Seasonality	-0.09	0.062
p2m3 *	Precipitation Seasonality	-0.09	0.062
p2m5 *	Precipitation Seasonality	-0.14*	0.062
p2m6 *	Precipitation Seasonality	0.39***	0.062
p3m1 *	Precipitation Seasonality	0.06	0.062
p3m2 *	Precipitation Seasonality	0.11	0.062
p3m3 *	Precipitation Seasonality	0.11	0.062
p3m4 *	Precipitation Seasonality	0.06	0.062
p3m5 *	Precipitation Seasonality	0.29***	0.062
p3m6 *	Precipitation Seasonality	-0.04	0.062
p3m7 *	Precipitation Seasonality	0.06	0.062
p4m1 *	Precipitation Seasonality	0.00	0.062
p4m2 *	Precipitation Seasonality	-0.09	0.062
p4m3 *	Precipitation Seasonality	0.06	0.062
p4m4 *	Precipitation Seasonality	0.00	0.062
p4m5 *	Precipitation Seasonality	-0.09	0.062
p4m6 *	Precipitation Seasonality	0.43***	0.062
p4m7 *	Precipitation Seasonality	0.00	0.062
p5m2 *	Precipitation Seasonality	-0.09	0.062
p5m3 *	Precipitation Seasonality	-0.09	0.062
p5m5 *	Precipitation Seasonality	-0.14*	0.062
p5m6 *	Precipitation Seasonality	0.39***	0.062
p6m1 *	Precipitation Seasonality	0.22***	0.062
p6m2 *	Precipitation Seasonality	0.19**	0.062
p6m3 *	Precipitation Seasonality	0.32***	0.062
p6m4 *	Precipitation Seasonality	0.22***	0.062
p6m5 *	Precipitation Seasonality	-0.20**	0.062
p6m6 *	Precipitation Seasonality	0.29***	0.062
p6m7 *	Precipitation Seasonality	0.22***	0.062
p7m1 *	Precipitation Seasonality	0.02	0.062
p7m2 *	Precipitation Seasonality	-0.03	0.062
p7m3 *	Precipitation Seasonality	0.09	0.062
p7m4 *	Precipitation Seasonality	0.02	0.062
p7m5 *	Precipitation Seasonality	-0.10	0.062
p7m6 *	Precipitation Seasonality	0.40***	0.062
p7m7 *	Precipitation Seasonality	0.02	0.062

¹*p<0.05; **p<0.01; ***p<0.001

²SE = Standard Error

Source: Article Notebook

Table 2: Linear regression analysis of the relationship between Functional Trophic Asymmetry and Network Specialization. Statistically significant effects (p<0.05) are marked with (*). Beta correspond to the variable effect coefficient in the model and SE correspond to the standard error.

Characteristic	Beta ¹	SE ²
FTA (mean)	3.3***	0.327
FTA (sd)	-1.0***	0.137

¹*p<0.05; **p<0.01; ***p<0.001

²SE = Standard Error

Source: Article Notebook

538 **6 References**

- 539 Acevedo-Quintero, J. F., Zamora-Abrego, J. G., & García, D. (2020). From struc-
 540 ture to function in mutualistic interaction networks: Topologically important
 541 frugivores have greater potential as seed dispersers. *Journal of Animal Ecology*,
 542 89(9), 2181–2191.
- 543 Acevedo-Quintero, J. F., Saldaña-Vázquez, R. A., Mendoza, E., & Zamora-Abrego,
 544 J. G. (2020). Sampling bias affects the relationship between structural impor-
 545 tance and species body mass in frugivore-plant interaction networks. *Ecological
 546 Complexity*, 44, 100870.
- 547 Ackerly, D. D. (2003). Community assembly, niche conservatism, and adaptive evolu-
 548 tion in changing environments. *International Journal of Plant Sciences*, 164(S3),
 549 S165–S184.
- 550 Albrecht, J., Classen, A., Vollständt, M. G., Mayr, A., Mollel, N. P., Schellenberger
 551 Costa, D., et al. (2018). Plant and animal functional diversity drive mutualistic
 552 network assembly across an elevational gradient. *Nature Communications*, 9(1),
 553 3177.
- 554 Allesina, S., Alonso, D., & Pascual, M. (2008). A general model for food web struc-
 555 ture. *Science*, 320(5876), 658–661.
- 556 Antonelli, A., & Sanmartín, I. (2011). Why are there so many plant species in the
 557 neotropics? *Taxon*, 60(2), 403–414.
- 558 Bello, C., Schleuning, M., & Graham, C. H. (2023). Analyzing trophic ecosystem
 559 functions with the interaction functional space. *Trends in Ecology & Evolution*.
- 560 Bjorholm, S., Svenning, J.-C., Skov, F., & Balslev, H. (2005). Environmental and
 561 spatial controls of palm (arecaceae) species richness across the americas. *Global
 562 Ecology and Biogeography*, 14(5), 423–429.
- 563 Blüthgen, N., & Klein, A.-M. (2011). Functional complementarity and specialisa-
 564 tion: The role of biodiversity in plant–pollinator interactions. *Basic and Applied
 565 Ecology*, 12(4), 282–291.
- 566 Blüthgen, N., Menzel, F., & Blüthgen, N. (2006). Measuring specialization in species
 567 interaction networks. *BMC Ecology*, 6(1), 1–12.
- 568 Blüthgen, N., Menzel, F., Hovestadt, T., Fiala, B., & Blüthgen, N. (2007). Special-
 569 ization, constraints, and conflicting interests in mutualistic networks. *Current
 570 Biology*, 17(4), 341–346.
- 571 Bogoni, J. A., Peres, C. A., & Ferraz, K. M. (2020). Extent, intensity and drivers of
 572 mammal defaunation: A continental-scale analysis across the neotropics. *Sci-
 573 entific Reports*, 10(1), 14750.
- 574 Carstensen, D. W., Lessard, J.-P., Holt, B. G., Krabbe Borregaard, M., & Rahbek,
 575 C. (2013). Introducing the biogeographic species pool. *Ecography*, 36(12), 1310–
 576 1318.
- 577 Classen, A., Eardley, C. D., Hemp, A., Peters, M. K., Peters, R. S., Ssymank, A.,
 578 & Steffan-Dewenter, I. (2020). Specialization of plant–pollinator interactions
 579 increases with temperature at mt. kilimanjaro. *Ecology and Evolution*, 10(4),
 580 2182–2195.
- 581 Cornell, H. V., & Harrison, S. P. (2014). What are species pools and when are they
 582 important? *Annual Review of Ecology, Evolution, and Systematics*, 45(1), 45–67.
- 583 Dehling, D. M. (2018). The structure of ecological networks. *Ecological Networks in
 584 the Tropics: An Integrative Overview of Species Interactions From Some of the
 585 Most Species-Rich Habitats on Earth*, 29–42.
- 586 Dehling, D. M., Töpfer, T., Schaefer, H. M., Jordano, P., Böhning-Gaese, K., &
 587 Schleuning, M. (2014). Functional relationships beyond species richness pat-
 588 terns: Trait matching in plant–bird mutualisms across scales. *Global Ecology and
 589 Biogeography*, 23(10), 1085–1093.
- 590 Dehling, D. M., Peralta, G., Bender, I. M., Blendinger, P. G., Böhning-Gaese, K.,
 591 Muñoz, M. C., et al. (2020). Similar composition of functional roles in andean

- 592 seed-dispersal networks, despite high species and interaction turnover. *Ecology*,
 593 101(7), e03028.
- 594 Donoso, I., García, D., Martínez, D., Tylianakis, J. M., & Stouffer, D. B. (2017).
 595 Complementary effects of species abundances and ecological neighborhood on
 596 the occurrence of fruit-frugivore interactions. *Frontiers in Ecology and Evolution*,
 597 133.
- 598 Donoso, I., Sorensen, M. C., Blendinger, P. G., Kissling, W. D., Neuschulz, E. L.,
 599 Mueller, T., & Schleuning, M. (2020). Downsizing of animal communities trig-
 600 gers stronger functional than structural decay in seed-dispersal networks. *Nature
 Communications*, 11(1), 1582.
- 602 Dormann, C. F., Fründ, J., Blüthgen, N., & Gruber, B. (2009). Indices, graphs and
 603 null models: Analyzing bipartite ecological networks.
- 604 Durand-Bessart, C., Cordeiro, N. J., Chapman, C. A., Abernethy, K., Forget, P.-M.,
 605 Fontaine, C., & Bretagnolle, F. (2023). Trait matching and sampling effort shape
 606 the structure of the frugivory network in afrotropical forests. *New Phytologist*,
 607 237(4), 1446–1462.
- 608 Emer, C., Jordano, P., Pizo, M. A., Ribeiro, M. C., Silva, F. R. da, & Galetti, M.
 609 (2020). Seed dispersal networks in tropical forest fragments: Area effects, rem-
 610 nant species, and interaction diversity. *Biotropica*, 52(1), 81–89.
- 611 Fick, S. E., & Hijmans, R. J. (2017). WorldClim 2: New 1-km spatial resolution cli-
 612 mate surfaces for global land areas. *International Journal of Climatology*, 37(12),
 613 4302–4315.
- 614 García, D., Donoso, I., & Rodríguez-Pérez, J. (2018). Frugivore biodiversity and
 615 complementarity in interaction networks enhance landscape-scale seed dispersal
 616 function. *Functional Ecology*, 32(12), 2742–2752.
- 617 Gevrey, M., Dimopoulos, I., & Lek, S. (2003). Review and comparison of methods to
 618 study the contribution of variables in artificial neural network models. *Ecological
 Modelling*, 160(3), 249–264.
- 619 Guzman, L. M., Germain, R. M., Forbes, C., Straus, S., O'Connor, M. I., Gravel,
 620 D., et al. (2019). Towards a multi-trophic extension of metacommunity ecology.
 621 *Ecology Letters*, 22(1), 19–33.
- 622 Halpern, B. S., & Floeter, S. R. (2008). Functional diversity responses to changing
 623 species richness in reef fish communities. *Marine Ecology Progress Series*, 364,
 624 147–156.
- 625 HilleRisLambers, J., Adler, P. B., Harpole, W. S., Levine, J. M., & Mayfield, M. M.
 626 (2012). Rethinking community assembly through the lens of coexistence theory.
 627 *Annual Review of Ecology, Evolution, and Systematics*, 43, 227–248.
- 628 Hoekstra, F. A., Golovina, E. A., & Buitink, J. (2001). Mechanisms of plant desicca-
 629 tion tolerance. *Trends in Plant Science*, 6(9), 431–438.
- 630 Kissling, W. D., Dormann, C. F., Groeneveld, J., Hickler, T., Kühn, I., McInerny,
 631 G. J., et al. (2012). Towards novel approaches to modelling biotic interactions
 632 in multispecies assemblages at large spatial extents. *Journal of Biogeography*,
 633 39(12), 2163–2178.
- 634 Kissling, W. D., Balslev, H., Baker, W. J., Dransfield, J., Göldel, B., Lim, J. Y.,
 635 et al. (2019). PalmTraits 1.0, a species-level functional trait database of palms
 636 worldwide. *Scientific Data*, 6(1), 178.
- 637 Kraft, N. J., & Ackerly, D. D. (2010). Functional trait and phylogenetic tests of
 638 community assembly across spatial scales in an amazonian forest. *Ecological
 Monographs*, 80(3), 401–422.
- 639 Kraft, N. J., Valencia, R., & Ackerly, D. D. (2008). Functional traits and niche-
 640 based tree community assembly in an amazonian forest. *Science*, 322(5901),
 641 580–582.
- 642 Kraft, N. J., Adler, P. B., Godoy, O., James, E. C., Fuller, S., & Levine, J. M.
 643 (2015). Community assembly, coexistence and the environmental filtering
 644 metaphor. *Functional Ecology*, 29(5), 592–599.

- 647 Laliberté, E., & Legendre, P. (2010). A distance-based framework for measuring
 648 functional diversity from multiple traits. *Ecology*, 91(1), 299–305.
- 649 Lavorel, S., Storkey, J., Bardgett, R. D., De Bello, F., Berg, M. P., Le Roux, X., et
 650 al. (2013). A novel framework for linking functional diversity of plants with other
 651 trophic levels for the quantification of ecosystem services. *Journal of Vegetation
 652 Science*, 24(5), 942–948.
- 653 Lessard, J.-P., Belmaker, J., Myers, J. A., Chase, J. M., & Rahbek, C. (2012). Infer-
 654 ring local ecological processes amid species pool influences. *Trends in Ecology &
 655 Evolution*, 27(11), 600–607.
- 656 Lim, J. Y., Svenning, J.-C., Göldel, B., Faurby, S., & Kissling, W. D. (2020).
 657 Frugivore-fruit size relationships between palms and mammals reveal past and
 658 future defaunation impacts. *Nature Communications*, 11(1), 4904.
- 659 Marjakangas, E.-L., Muñoz, G., Turney, S., Albrecht, J., Neuschulz, E. L., Schleun-
 660 ing, M., & Lessard, J.-P. (2022). Trait-based inference of ecological network
 661 assembly: A conceptual framework and methodological toolbox. *Ecological
 662 Monographs*, 92(2), e1502.
- 663 Marques Draxler, C., & Kissling, W. D. (2022). The mutualism–antagonism con-
 664 tinuum in neotropical palm–frugivore interactions: From interaction outcomes to
 665 ecosystem dynamics. *Biological Reviews*, 97(2), 527–553.
- 666 McCain, C. M., & King, S. R. (2014). Body size and activity times mediate mam-
 667 malian responses to climate change. *Global Change Biology*, 20(6), 1760–1769.
- 668 McFadden, I. R., Fritz, S. A., Zimmermann, N. E., Pellissier, L., Kissling, W. D.,
 669 Tobias, J. A., et al. (2022). Global plant-frugivore trait matching is shaped by
 670 climate and biogeographic history. *Ecology Letters*, 25(3), 686–696.
- 671 Messeder, J. V. S., Guerra, T. J., Dátilo, W., & Silveira, F. A. (2020). Searching
 672 for keystone plant resources in fruit-frugivore interaction networks across the
 673 neotropics. *Biotropica*, 52(5), 857–870.
- 674 Moretti, M., & Legg, C. (2009). Combining plant and animal traits to assess commu-
 675 nity functional responses to disturbance. *Ecography*, 32(2), 299–309.
- 676 Morrone, J. J. (2014). Biogeographical regionalisation of the neotropical region.
 677 *Zootaxa*, 3782(1), 1–110.
- 678 Muñoz, G., Trøjelsgaard, K., & Kissling, W. D. (2019). A synthesis of animal-
 679 mediated seed dispersal of palms reveals distinct biogeographical differences
 680 in species interactions. *Journal of Biogeography*, 46(2), 466–484.
- 681 Nagy, D. D., Magura, T., Horváth, R., Debnár, Z., & Tóthmérész, B. (2018). Arthro-
 682 pod assemblages and functional responses along an urbanization gradient: A
 683 trait-based multi-taxa approach. *Urban Forestry & Urban Greening*, 30, 157–168.
- 684 Onstein, R. E., Carter, R. J., Xing, Y., & Linder, H. P. (2014). Diversification rate
 685 shifts in the cape floristic region: The right traits in the right place at the right
 686 time. *Perspectives in Plant Ecology, Evolution and Systematics*, 16(6), 331–340.
- 687 Onstein, R. E., Baker, W. J., Couvreur, T. L., Faurby, S., Svenning, J.-C., &
 688 Kissling, W. D. (2017). Frugivory-related traits promote speciation of tropical
 689 palms. *Nature Ecology & Evolution*, 1(12), 1903–1911.
- 690 Paine, C. T., Baraloto, C., Chave, J., & Hérault, B. (2011). Functional traits of indi-
 691 vidual trees reveal ecological constraints on community assembly in tropical rain
 692 forests. *Oikos*, 120(5), 720–727.
- 693 Peña, R., Schleuning, M., Dalerum, F., Donoso, I., Rodríguez-Pérez, J., & García,
 694 D. (2023). Abundance and trait-matching both shape interaction frequencies
 695 between plants and birds in seed-dispersal networks. *Basic and Applied Ecology*,
 696 66, 11–21.
- 697 Poisot, T. (2023). Guidelines for the prediction of species interactions through bi-
 698 nary classification. *Methods in Ecology and Evolution*, 14(5), 1333–1345.
- 699 Poisot, T., Stouffer, D. B., & Kéfi, S. (2016). Describe, understand and predict.
 700 *Functional Ecology*, 30(12), 1878–1882.

- Poisot, T., Bergeron, G., Cazelles, K., Dallas, T., Gravel, D., MacDonald, A., et al. (2021). Global knowledge gaps in species interaction networks data. *Journal of Biogeography*, 48(7), 1552–1563.
- Préau, C., Dubos, N., Lenormand, M., Denelle, P., Le Louarn, M., Alleaume, S., & Luque, S. (2022). Dispersal-based species pools as sources of connectivity area mismatches. *Landscape Ecology*, 1–15.
- Pyron, R. A., Costa, G. C., Patten, M. A., & Burbrink, F. T. (2015). Phylogenetic niche conservatism and the evolutionary basis of ecological speciation. *Biological Reviews*, 90(4), 1248–1262.
- Rohr, R. P., Scherer, H., Kehrli, P., Mazza, C., & Bersier, L.-F. (2010). Modeling food webs: Exploring unexplained structure using latent traits. *The American Naturalist*, 176(2), 170–177.
- Saravia, L. A., Marina, T. I., Kristensen, N. P., De Troch, M., & Momo, F. R. (2022). Ecological network assembly: How the regional metaweb influences local food webs. *Journal of Animal Ecology*, 91(3), 630–642.
- Schlägel, U. E., Grimm, V., Blaum, N., Colangeli, P., Dammhahn, M., Eccard, J. A., et al. (2020). Movement-mediated community assembly and coexistence. *Biological Reviews*, 95(4), 1073–1096.
- Schleuning, M., Fründ, J., Klein, A.-M., Abrahamszyk, S., Alarcón, R., Albrecht, M., et al. (2012). Specialization of mutualistic interaction networks decreases toward tropical latitudes. *Current Biology*, 22(20), 1925–1931.
- Schleuning, M., Ingmann, L., Strauss, R., Fritz, S. A., Dalsgaard, B., Matthias Dehling, D., et al. (2014). Ecological, historical and evolutionary determinants of modularity in weighted seed-dispersal networks. *Ecology Letters*, 17(4), 454–463.
- Schleuning, M., Fründ, J., Schweiger, O., Welk, E., Albrecht, J., Albrecht, M., et al. (2016). Ecological networks are more sensitive to plant than to animal extinction under climate change. *Nature Communications*, 7(1), 13965.
- Schleuning, M., Neuschulz, E. L., Albrecht, J., Bender, I. M., Bowler, D. E., Dehling, D. M., et al. (2020). Trait-based assessments of climate-change impacts on interacting species. *Trends in Ecology & Evolution*, 35(4), 319–328.
- Schleuning, M., García, D., & Tobias, J. A. (2023). Animal functional traits: Towards a trait-based ecology for whole ecosystems. *Functional Ecology*. Wiley Online Library.
- Seibold, S., Cadotte, M. W., MacIvor, J. S., Thorn, S., & Müller, J. (2018). The necessity of multitrophic approaches in community ecology. *Trends in Ecology & Evolution*, 33(10), 754–764.
- Strydom, T., Bouskila, S., Banville, F., Barros, C., Caron, D., Farrell, M. J., et al. (2022). Food web reconstruction through phylogenetic transfer of low-rank network representation. *Methods in Ecology and Evolution*, 13(12), 2838–2849.
- Terry, J. C. D., & Lewis, O. T. (2020). Finding missing links in interaction networks. *Ecology*, 101(7), e03047.
- Thuiller, W., Calderón-Sanou, I., Chalmandrier, L., Gaüzère, P., O'Connor, L. M., Ohlmann, M., et al. (2024). Navigating the integration of biotic interactions in biogeography. *Journal of Biogeography*, 51(4), 550–559.
- Villéger, S., Mason, N. W., & Mouillot, D. (2008). New multidimensional functional diversity indices for a multifaceted framework in functional ecology. *Ecology*, 89(8), 2290–2301.
- Webb, S. D. (2006). The great american biotic interchange: Patterns and processes. *Annals of the Missouri Botanical Garden*, 93(2), 245–257.
- Whiteman-Jennings, W. (2015). INTO THE TROPICS: A QUANTITATIVE STUDY OF MAMMALS IN THE GREAT AMERICAN BIOTIC INTERCHANGE.
- Wiens, J. J., & Graham, C. H. (2005). Niche conservatism: Integrating evolution, ecology, and conservation biology. *Annu. Rev. Ecol. Evol. Syst.*, 36, 519–539.

- 755 Wilman, H., Belmaker, J., Simpson, J., Rosa, C. de la, Rivadeneira, M. M., & Jetz,
 756 W. (2014). Elton Traits 1.0: Species-level foraging attributes of the world's birds
 757 and mammals: Ecological archives E095-178. *Ecology*, 95(7), 2027–2027.
 758 Zona, S., & Henderson, A. (1989). A review of animal-mediated seed dispersal of
 759 palms. *Selbyana*, 6–21.

760 **7 Supplementary Material**
 761 **7.1 Supplementary figures**

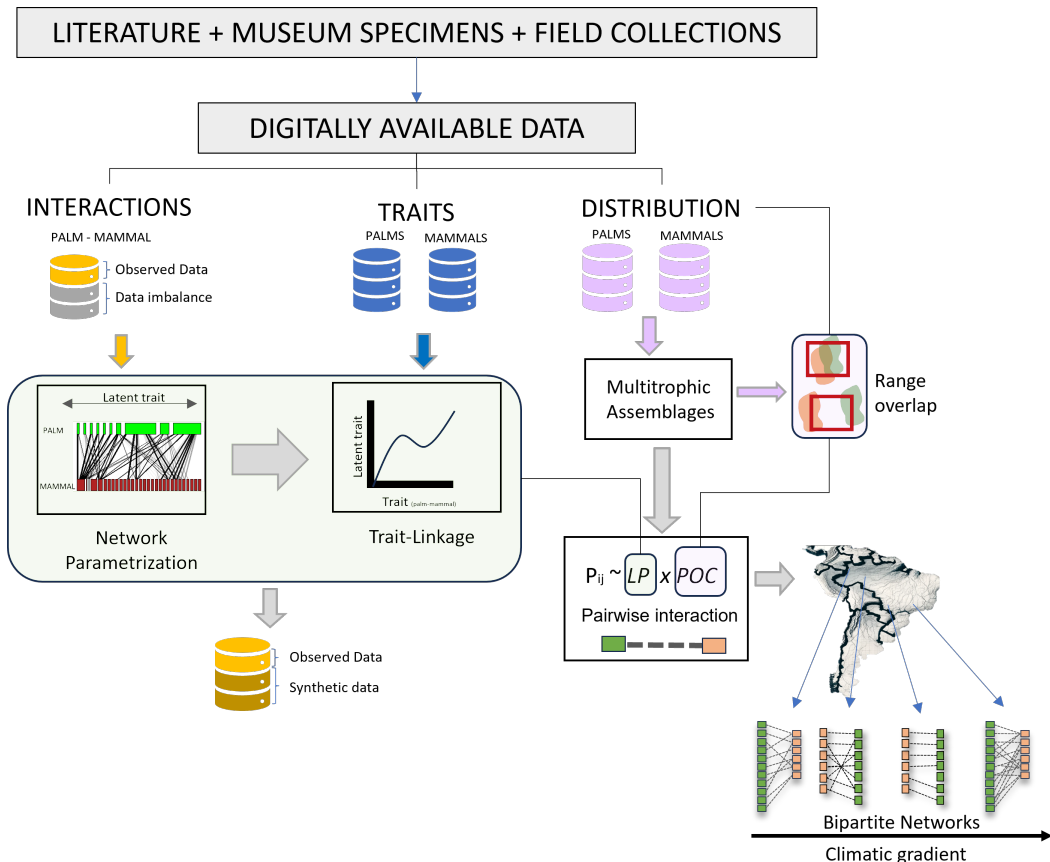


Figure 4: Figure S1: A comprehensive workflow designed to integrate and harmonize primary biodiversity data from digitally accessible datasets. In our case study, these datasets are systematically categorized into three key components: palm-mammal interactions, species traits, and geographical distribution. The workflow is structured to address data imbalances through network parametrization, which ensures that underrepresented data is appropriately synthesized to generate a more balanced dataset. Additionally, trait-linkage analysis is employed to examine relationships between latent traits, facilitating a deeper understanding of species interactions. Further, we examine the assembly of multitrophic networks, which are constructed based on their matching traits and the spatial overlap of species distributions. Ultimately, these networks can provide insights on the drivers of network assembly across diverse environmental gradients.

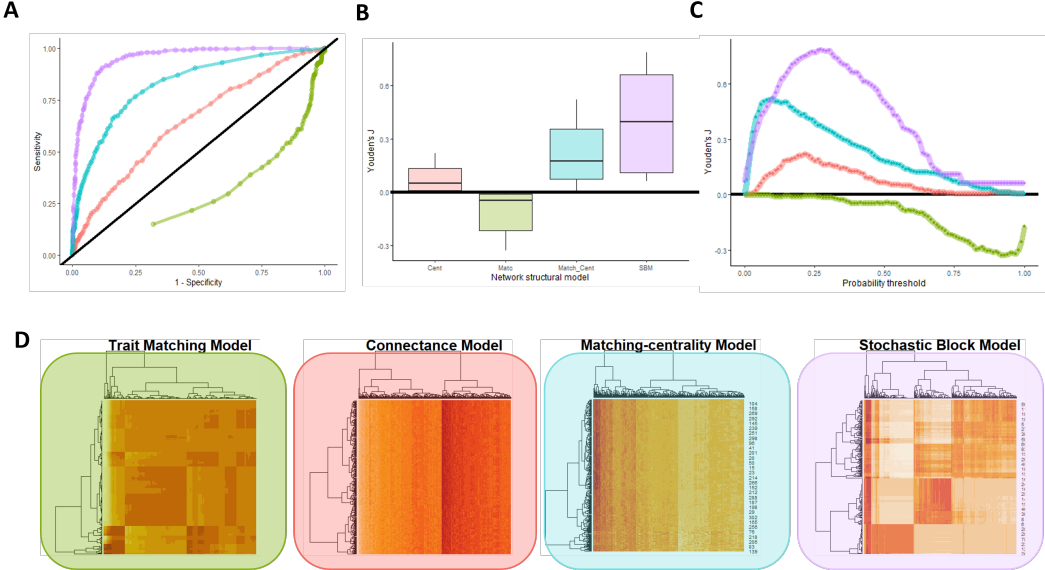


Figure 5: Figure S2: Evaluating distinct network structural models to predict mutualistic interactions between palms and mammals in the Neotropics. **(A) Receiver Operating Characteristic (ROC) Curves:** This panel illustrates the performance of different network structural models in predicting interactions across species pairs. Each curve is color-coded to represent a distinct model, providing insight into the trade-off between true positive and false positive rates across varying thresholds. **(B) Boxplots of Model Accuracy:** This panel compares the accuracy of the models, displaying the distribution of accuracy scores across multiple datasets or iterative simulations. The variability, indicated by the spread of the boxplots, highlights the consistency and reliability of each model's predictions. **(C) Precision-Recall (PR) Curves:** This panel focuses on the trade-offs between precision and recall (evaluated with Youden's J) at different probability thresholds for each model. The curves help to identify the most effective models in minimizing false positives while maximizing true positives, especially in imbalanced datasets such as ours where interactions are sparse. **(D) Heatmaps of Predicted Adjacency Matrices:** This panel visualizes the predicted interactions in the form of adjacency matrices for the four distinct models examined in this study: the Trait Matching Model, Connectance Model, Matching-centrality Model, and Stochastic Block Model. Hierarchical clustering applied to species based on their predicted interactions helps in elucidating the structural differences between models, revealing patterns of species clustering and potential interaction modules.

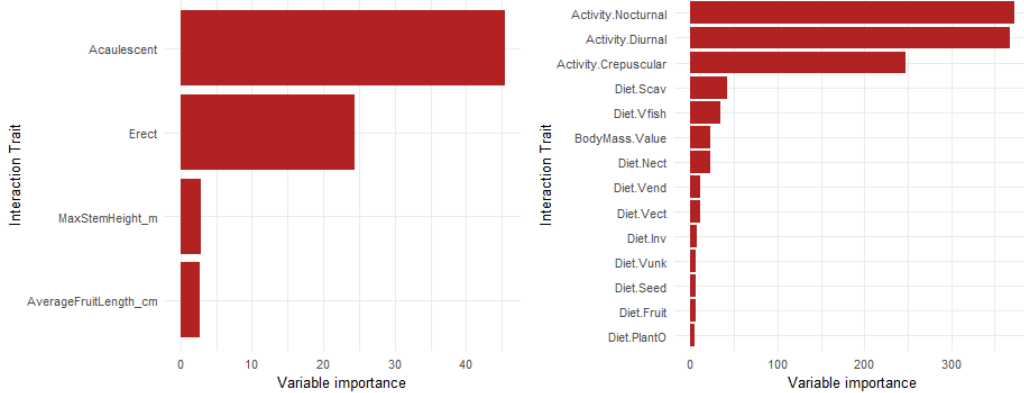


Figure 6: Figure S3: Variable Importance for Interaction Traits in Palm and Mammal frugivores. The left panel presents the relative importance of palm interaction traits, where *Acaulescent* and *Erect* growth forms are identified as the most influential traits to define interactions with mammals. Secondary traits such as *MaxStemHeight_m* and *AverageFruitLength_cm* contribute moderately to delineate interactions. The right panel shows the importance of mammal interaction traits in shaping their interactions with palms, with activity patterns—nocturnal and diurnal—emerging as the most critical. Crepuscular activity also shows notable relevance. Among diet-related traits, scavenging and fish consumption, alongside body mass, are recognized as important, though their influence is comparatively lower.

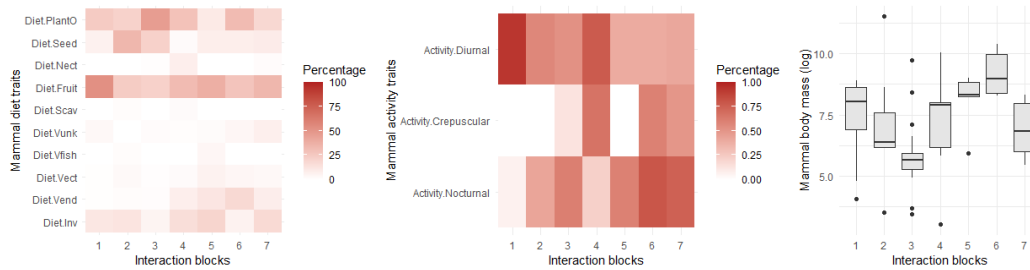


Figure 7: Figure S4: Mammal trait representations across SBM groups (interaction blocks). **Dietary Traits (Left Panel):** The heatmap illustrates the percentage distribution of various mammalian diet types across the interaction blocks (SBM groups). Darker shades indicate a higher prevalence of specific diet types within particular blocks. This distribution reveals the trophic specialization of mammals and suggests how different diet types are clustered or dispersed across ecological interactions. **Activity Patterns (Middle Panel):** The second heatmap focuses on mammalian activity data, categorized as Diurnal, Crepuscular, and Nocturnal. Darker shades signify higher percentages, allowing for a comparison of how activity patterns are distributed across the same interaction blocks. This panel helps in understanding temporal niche partitioning and its relationship to ecological interactions. **Body Mass Variation (Right Panel):** The boxplot illustrates the distribution of mammalian body mass (log-transformed) across the interaction blocks.

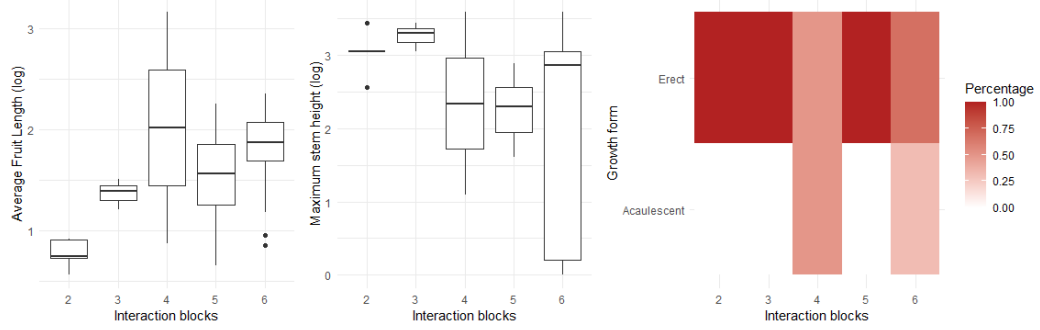


Figure 8: Figure S5: **Palm trait representations across SBM groups (interaction blocks)**. The left and middle panels feature boxplots that display the log-transformed average fruit length and maximum stem height, respectively, for each interaction block. The right panel shows the relative proportions of plant growth forms within each interaction block. The color gradient represents the percentage contribution of each growth form.

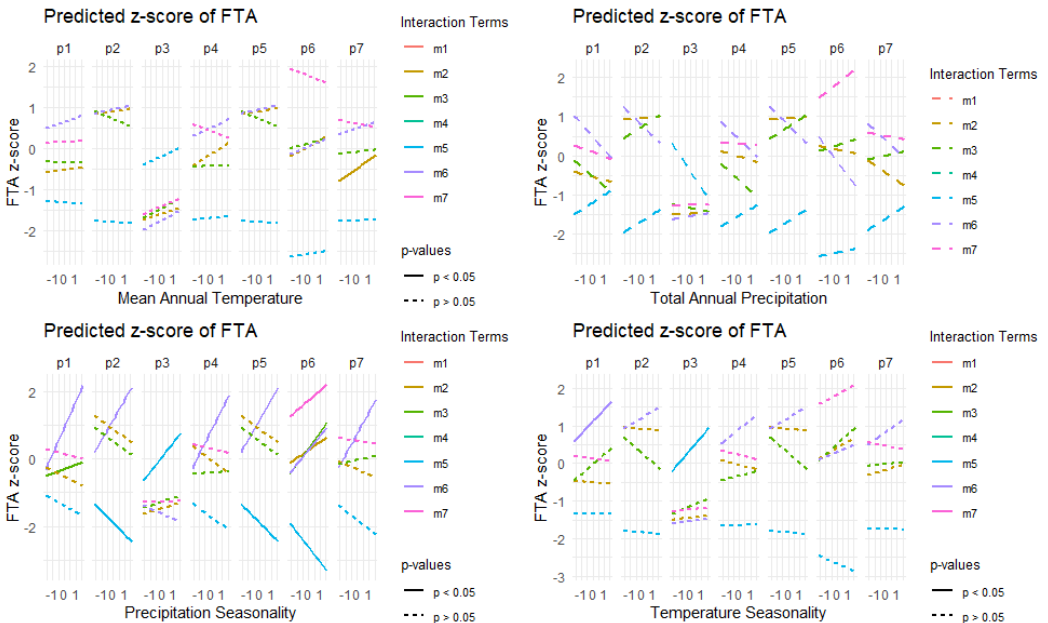


Figure 9: Figure S6: **Predicted z-scores of FTA (Functional Trait Assemblage) as a function of four climate variables and across combinations of seven different palm (p1 to p7) and seven mammal (m1 to m7) SBM groups**. The four panels represent: Mean Annual Temperature (top left), Total Annual Precipitation (top right), Precipitation Seasonality (bottom left), and Temperature Seasonality (bottom right). Solid lines indicate statistically significant relationships ($p < 0.05$), while dashed lines indicate non-significant relationships ($p \geq 0.05$). The different interaction models are color-coded as indicated in the legend and the facet title.

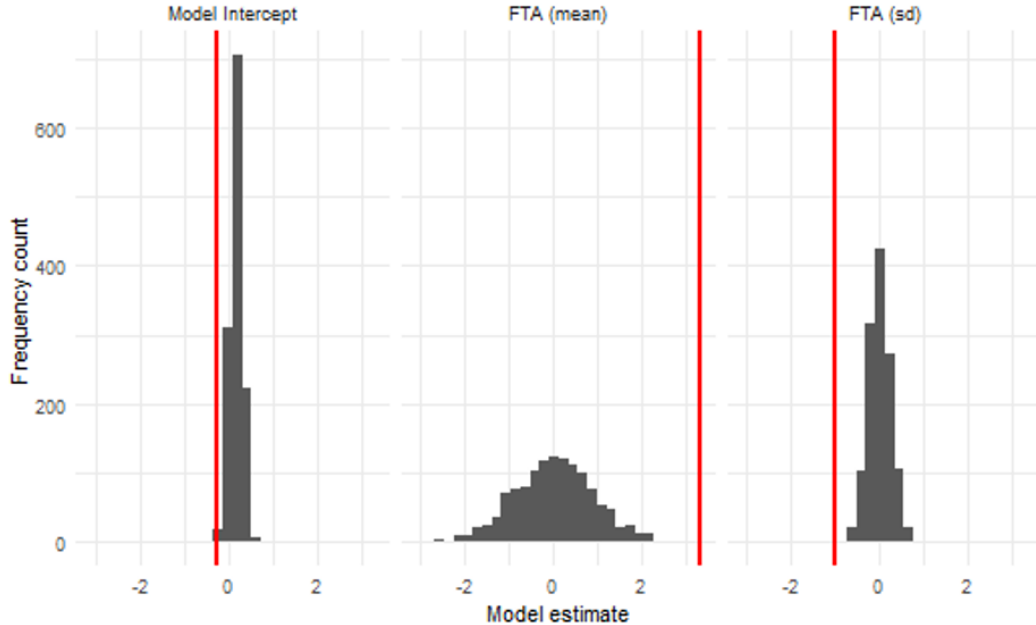


Figure 10: Figure S7: **Frequency distribution of model estimates for the intercept and Functional Trait Asymmetry (FTA) metrics.** The three panels display the distribution of model estimates for the intercept (left), FTA mean (center), and FTA standard deviation (right). Red vertical lines denote the actual estimates obtained from the model, serving as a reference point against the resampled or bootstrapped estimate distributions. The histograms illustrate the frequency count of estimates derived from a null model that reshuffled species co-occurrences. FTA mean is the mean FTA z-scores for all SBM palm-mammal group combinations in a gridcell. FTA sd is the standard deviation of the distribution of FTA z-scores for all SBM palm-mammal group combinations in a gridcell

762 7.2 Supplementary text

763 764 Supplementary text S1: Additional details about the structural network models used to predict species interactions in this study

765 To capture probabilistic patterns from interactions observed at the continental scale,
766 we tested four assembly models: the stochastic block model (SBM), the connectance
767 model, the matching-trait model, and the matching-centrality model. Each model
768 was evaluated based on its ability to predict interaction probabilities between palm
769 and mammal species pairs.

770 • 1. Stochastic Block Model (SBM):

771 The SBM assumes that ecological networks exhibit a modular pattern, where
772 subsets of species interact more within their groups of highly connected
773 species (Terry and Lewis, 2020).

774 The model generates an incidence matrix, (Z), reflecting species-level associations
775 to a group, and a squared matrix, (Θ), reflecting the interaction probabilities within
776 and between groups. The likelihood (L) of the SBM is given by:

$$L = \prod_{i,j} \left(\Theta_{Z_i Z_j} \right)^{A_{ij}} \left(1 - \Theta_{Z_i Z_j} \right)^{1-A_{ij}}$$

777 where

- 778 • (A) is the adjacency matrix of observed interactions,
- 779 • (Z_i)(Z_j) are the group memberships of species (i) and (j), and
- 780 • ($\Theta_{Z_i Z_j}$) is the probability of interaction between groups (Z_i) and (Z_j).

781 • **2. Connectance Model:**

782 The connectance model posits that the interactions of specialist species are subsets
 783 of those of generalist species. It optimizes connectivity scores, (C_i), assigned to
 784 species to maximize the likelihood of recreating the observed network pattern. The
 785 likelihood (L) for this model is:

$$L = \prod_{i,j} (C_i \cdot C_j)^{A_{ij}} (1 - C_i \cdot C_j)^{1-A_{ij}}$$

786 where (C_i) is the connectivity score of species (i).

787 • **3. Matching-Trait Model:**

788 The matching-trait model assumes that species interactions are not random but
 789 based on trait differences. It optimizes parameters by scoring interactions along one
 790 or multiple latent-trait axes. The interaction probability (P_{ij}) between species (i)
 791 and (j) is determined by:

$$P_{ij} = f(T_i, T_j)$$

792 where (T_i) and (T_j) are trait vectors for species (i) and (j), and (f) is a function
 793 measuring trait similarity or compatibility.

794 • **4. Matching-Centrality Model:**

795 The matching-centrality model combines the approaches of the connectance and
 796 matching-trait models. It optimizes both species connectivity scores and latent trait
 797 axes. The likelihood (L) for this model is:

$$L = \prod_{i,j} (C_i \cdot C_j \cdot f(T_i, T_j))^{A_{ij}} (1 - C_i \cdot C_j \cdot f(T_i, T_j))^{1-A_{ij}}$$

798 Following the guidelines established by Poisot (2023), Youden's J statistic was used
 799 to compare model performance. Youden's J is a metric of model informedness that
 800 balances sensitivity and specificity, calculated as:

$$J = \text{Sensitivity} + \text{Specificity} - 1$$

801 **8 Data Accessibility Statement**

802 Data is open-source, digitally available at their respective sources.

803 **9 Conflict of Interest Statement**

804 The authors declare no conflict of interest.